Do Hydration Dynamics Follow the Structural Perturbation during Thermal Denaturation of a Protein: A Terahertz Absorption Study

Trung Quan Luong,[†] Pramod Kumar Verma,[‡] Rajib Kumar Mitra,[‡] and Martina Havenith[†]*
[†]Department of Physical Chemistry II, Ruhr-University Bochum, Bochum, Germany; and [‡]Unit for Nano-Science and Technology, Department of Chemical, Biological and Macromolecular Sciences, S.N. Bose National Centre for Basic Sciences, Salt Lake, Kolkata, India

ABSTRACT We investigate the thermal denaturation of human serum albumin and the associated solvation using terahertz (THz) spectroscopy in aqueous buffer solution. Far- and near-ultraviolet circular dichroism spectroscopy reveal that the protein undergoes a native (N) to extended (E) state transition at temperature $\leq 55^{\circ}$C with a marginal change in the secondary and tertiary structure. At 70°C, the protein transforms into an unfolded (U) state with significant irreversible disruption of its structures. We measure the concentration- and temperature-dependent THz absorption coefficient (α) of the protein solution using a p-Ge THz difference spectrometer (2.1–2.8 THz frequency range), thereby probing the collective protein-water network dynamics. When the solvated protein is heated up to 55°C and cooled down again, a reversible change in THz absorption is observed. When increasing the temperature up to 70°C, we find a dramatic irreversible change of THz absorption. The increase in THz absorption compared to bulk water is attributed to a blue shift in the spectrum of the solvated protein compared to bulk water. This is supported by measurements of THz absorption coefficients using THz time-domain spectroscopy (0.1–1.2 THz frequency range). We also use picosecond-resolved fluorescence spectroscopy of the tryptophan 214 moiety of human serum albumin. All experimental observations can be explained by a change in the hydration dynamics of the solvated protein due to the additional exposure of hydrophobic residues upon unfolding.

INTRODUCTION

Water is the lubricant of life. Despite the fact that all life takes place in water, the role of water is still underrated. Water's flexible hydrogen-bond network enables it to adapt its structure and dynamics to biological macromolecules. Water can interact with biomolecules by donating and accepting hydrogen bonds, by weaker van der Waals interactions, and/or via electrostatic steering. Hydration water makes significant contributions to the structure and energy of proteins and provides a responsive surrounding which enables conformational changes (1–3). However, water is not just a passive spectator solvent in biological processes, but is thought to have a vital function in most biomolecular and cellular processes (4–7). In particular, water may hold the key to the way proteins interact, (mis) fold, bind substrates, and aggregate. Self-assembly of proteins is controlled by a delicate interplay between hydrophobic and hydrophilic interactions. Water at protein interfaces (hydration water or interfacial water) has been shown to thermodynamically stabilize the native structure of biomacromolecules, to affect protein flexibility, and to contribute to molecular recognition in enzyme catalysis.

The hydrophobic effect which stems from the unfavorable interaction between water and the hydrophobic moiety of amino acids is assumed to play an important role in protein folding (8). Changes in physical and/or chemical parameters like temperature, pH, ionic strength, and addition of denaturating agents unfold the closely packed tertiary native structure of proteins. The essential role of hydration during the folding/unfolding process of protein has been studied using various techniques (9–14). Recently, terahertz (THz) absorption spectroscopy has been introduced as a new tool which is able to probe, label free, the change in collective protein-water network motions of hydrated biomolecular solutes involving several hydration shells (>10 Å) in the subpicosecond-to-picosecond timescale (15–20). The hydrogen-bonding network motions of water have absorption peaks in the frequency range between 1 and 6 THz (21–23). 1 THz is equivalent to a wavenumber of 33.3 cm^{-1}, or a wavelength of 300 μm. THz spectroscopy probes directly the collective intermolecular vibration of the hydrogen bond network, and is thus able to detect sensitively any solute-induced changes in the solvation dynamics. THz spectroscopy monitors the collective water network motions on the timescale of subpicosecond whereas other techniques detect processes on the nanosecond-to-microsecond timescale (NMR) or measure static properties (x ray).

Previously, the application of THz spectroscopy to study solvated biomolecules was hampered by the huge absorption of water in this frequency range, along with the lack of strong THz emitters. Therefore, most of the previous work reported in this frequency range involves dry protein powder or protein gel palates (24,25), which in turn questions the structural and functional integrity of the dehydrated protein itself. Our group has recently initiated the study of dynamical characterization of fully solvated small solutes and biomolecules in the THz range using a strong table-top THz source of a p-Ge THz difference spectrometer

(16–20,26). These studies showed that the absorption coefficient of water in the hydration shell of proteins and biomolecules differs significantly from that of bulk water in this frequency range. It is thus interesting to observe how the hydration dynamics of a protein responds upon unfolding and refolding.

In a combined experimental and molecular dynamics simulation study of our group (27) we could show that the observed changes in the THz absorption of the solvated protein can be explained by a blue shift of the water THz modes in the dynamical hydration shell, which can be directly related to a significant retardation of water dynamics. In this study, we predicted a decrease of the THz absorption of the protein solution compared to buffer at frequencies below 1.7 THz, whereas an increased absorption is predicted for frequencies above 1.7 THz. Both predictions have been confirmed by measurements.

In this report, we investigate the thermal denaturation of human serum albumin (HSA) fully dissolved in aqueous buffer solution, as reported by combining THz absorption spectroscopy with circular dichroism (CD) and fluorescence spectroscopy.

HSA is an important protein of the human body which acts as a transporter of fatty acids and for binding a great variety of metabolites, drugs, and organic compounds in the circulatory system (28). The crystal structure of this protein in its native state is well documented in the literature (29,30). It consists of a single polypeptide chain containing 585 amino acids. Under physiological condition (pH = 7) it adopts a heart-shaped three-dimensional structure with three homologous domains I–III, with each domain consisting of two subdomains A and B containing four and six α-helices, respectively. Thermal denaturation of this protein has previously been studied using different techniques (31–38). One of the early studies (35) concluded that thermal denaturation of this protein follows multiple steps: native (N) $\rightarrow$ extended (E) $\rightarrow$ unfolded (U). The study revealed that in the extended form (E) at $\leq$55°C, domains II and I move apart while almost keeping the native conformation intact. In contrast, in the unfolded state (U) domain II starts to melt, which is accompanied by a disruption of secondary and tertiary structure of the protein.

In this article, we measure the change in the coupled protein hydration dynamics of HSA upon denaturation using both time-domain and high power THz spectroscopy. The temperature of the native protein was increased stepwise from 20°C to 55°C (extended state), subsequently, the system was allowed to cool to 20°C (Process 1). In a second experiment, the protein was heated to 70°C (unfolded state) and then allowed to cool to 20°C (Process 2). Both processes are monitored using far- and near-ultraviolet (UV) CD spectroscopy, THz absorption using p-Ge laser in the frequency range of 2.1–2.8 THz, THz time-domain spectroscopy (THz-TDS) in the frequency range of 0.1–1.2 THz, and time-resolved fluorescence spectroscopy of the intrinsic fluorescence of the tryptophan (Trp) moiety of the protein with the major focus on the alteration of the coupled protein hydration dynamics. This study is, to our knowledge, the first one to investigate the effect of thermal denaturation of a protein using THz spectroscopy.

MATERIAL AND METHODS

Far-and near-UV CD measurements were performed with a model No. 815 spectrometer (JASCO, Oklahoma City, OK). We used our p-Ge difference spectrometer to record the integrated absorption of protein solution relative to buffer in the frequency range from 2.1 to 2.8 THz as a function of temperature. The frequency-dependent absorption coefficient $\alpha(\nu)$ and index of refraction $n(\nu)$ in the frequency range from 0.1 to 1.2 THz were obtained from measurements using a THz-TD spectrometer. Steady-state emission was measured with a Fluorolog fluorimeter (Horiba-Jobin Yvon, Edison, NJ) with a Peltier attachment to control the temperature. For the time-resolved measurements, we used a femtosecond-coupled time-correlated single-photon counting setup. The details of the instrumentation of CD, THz, and fluorescence spectrometer can be found in the Supporting Material.

Human serum albumin (HSA) protein was purchased from Sigma Aldrich (St. Louis, MO) at 99% or higher purity and was used without further purification. Protein solutions were prepared by dissolving proteins in phosphate-buffered saline (PBS) at pH 7.4 at required concentrations. The transmitted intensities in THz range were measured at a fixed layer thickness by using a standard liquid sample cell (model No. A145; Bruker Optics, Ettlingen, Germany) with a Teflon (Dupont, Wilmington, DE) spacer and z-cut quartz windows. The layer thickness of the aqueous sample, which was placed between two parallel quartz windows, was determined to be 52.6 $\pm$ 0.3 μm (using Fourier transform infrared spectroscopy to record the Etalon fringes). For all measurements, the temperatures of the samples were controlled by a thermostat. We allowed for thermal equilibration (temperature at $\pm$0.2°C around the temperature set value) for at least 10 min before the data were collected. For THz measurements with p-Ge laser and THz-TD spectrometer, the whole THz setup is enclosed in a chamber purged with dry air, keeping the humidity at 5% to reduce water vapor absorption.

RESULTS AND DISCUSSION

We have recorded the far-UV CD measurements of HSA between 200 and 260 nm as a function of temperature to probe changes in the secondary structure of the protein upon heating. The results are shown in Fig. 1 *A*. At 20°C the protein retains its native structure, with two characteristic peaks at 208 and 222 nm. We obtain 63.4% of α-helix, 12.6% of β-sheet, and 24% of other structural elements for the native structure which is in good agreement with previously reported studies (38–40). As the temperature is increased, the CD signal at 222 nm decreases, indicating a loss of α-helical content. In Fig. 1 *A* (*inset*), we display the optical rotation at 222 nm as a function of temperature. The change in the ellipticity at this wavelength serves as a probe for the α-helical content. As can be observed from the inset, the α-helix content decreases at 40°C to 61.5% (13.0% β-sheet and 25.5% other structures).

At 55°C, we obtain an α-helix content of 57.8%. When cooling down from 55°C to room temperature, the native spectrum is recovered (not shown here). Upon increasing

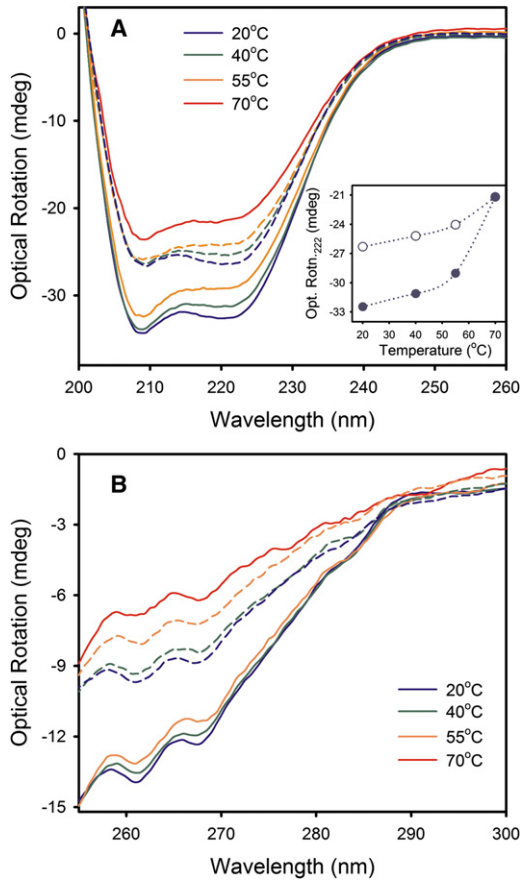

FIGURE 1 Far-UV (*A*) and near-UV (*B*) circular dichroism (CD) spectra of HSA in aqueous PBS buffer at different temperatures. (*Solid lines*) Thermal unfolding (forward, heating) process. (*Dashed lines*) Refolding (reverse, cooling) process. (*A*, *inset*) The change in the optical rotation at 222 nm for both heating (*solid symbols*) and cooling (*open symbols*) processes. (*Dotted lines*) Guide to the eyes.

the temperature to 70°C, a drastic irreversible change in the CD signal is observed. At 70°C, the content of α-helix is decreased to 41.4% (16% β-sheet and 42.6% of other conformers), which is in good agreement with 44% α-helix content at 65°C as reported by Moriyama and Takeda (41). The drastic change in the α-helix content corroborates the native (N) to unfolded (U) state transition of the protein. By subsequent cooling, part of the secondary structure is recovered. When cooled to 20°C, we obtain 46% α-helix structure (15% β-sheet and 39% of random coil), which proofs the irreversibility of the unfolding process (Fig. 1 *A*). It can be noted here that the β-sheet content of the protein does not change much upon refolding; however, that of the random coil increases considerably. This indicates a helix-to-coil transition at elevated temperature, as has been previously observed in the case of pH-induced denaturation (40).

To study the structural alteration in more detail, CD measurements in the near-UV region (250–300 nm) that reveal the tertiary structure of the protein are carried out as a function of temperature. The results are shown in Fig. 1 *B*. The observed CD spectrum at 20°C is in agreement with previous results which report two distinct peaks at 262 and 268 nm along with a shoulder at 280 nm (38–40,42). As the temperature is increased to 55°C, all spectral features remain intact; however, a decrease of the signals at 262 and 268 nm indicates a slight perturbation of the disulfide bridges (43,44). The insignificant change in the shoulder at 280-nm region is attributed to marginal changes in the Trp environment, as also supported by fluorescence measurements (see later). When increasing the temperature to 70°C, the CD spectrum is significantly altered in the frequency regions at 262 and 268 nm, indicating a rupture of many of the disulfide bonds. After cooling to 20°C, the CD spectrum is not recovered, indicating an irreversible structural perturbation during N→U transition.

THz spectroscopy has proven to be a new tool to study hydration dynamics of solvated protein (16,27). We have recorded the integrated THz absorption spectra of HSA solutions at 2.1–2.8 THz using the p-Ge THz difference spectrometer for concentrations up to 1.4 mM. The measurements were carried out at 20, 40, 55, and 70°C. The results are shown in Fig. 2. We find a decrease of the relative THz absorption coefficient with increasing concentration of the protein. In general a decrease in THz absorption, i.e., a THz defect, is expected in the case that highly absorbing water molecules in buffer (Fig. 3 *A*, *inset*) are replaced by less absorbing protein molecules (18). Considering the replacement of water by protein, the absorption coefficient of the protein solution can be calculated according to a two-component model as

$$\alpha_s = \alpha_b \frac{V_b}{V_T} + \alpha_p \frac{V_p}{V_T}, \tag{1}$$

where α_s, α_b, and α_p are the absorption coefficient of the protein solution, buffer, and protein, respectively, and V_b,

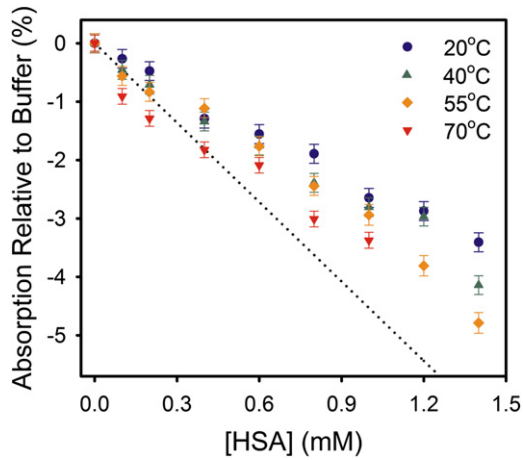

FIGURE 2 Concentration-dependent THz absorption relative to buffer of HSA in PBS buffer at four different temperatures measured with a p-Ge THz spectrometer in the range of 2.1–2.8 THz. (*Dotted line*) Two-component water displacement model.

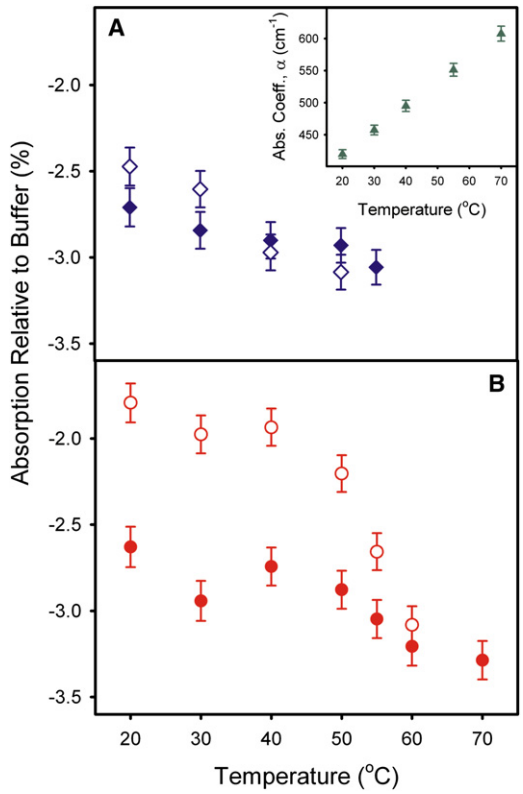

FIGURE 3 Temperature-dependent THz absorption relative to buffer for 1 mM HSA in PBS buffer for N-E transition (*A*) and N-U transition (*B*). (*Solid symbols*) Heating (unfolding) process; (*open symbols*) cooling (refolding) process. (*Inset*) Temperature-dependent absorption coefficient of PBS buffer.

V_p, and V_T are the volume of buffer, volume of protein, and total volume of the protein solution, respectively. The water displacement or change in the absorption coefficient of the protein solution relative to buffer (α_{relative}) can be calculated as

$$\alpha_{\text{relative}} = \frac{\alpha_s - \alpha_b}{\alpha_b} = \frac{V_b}{V_T} + \frac{\alpha_p}{\alpha_b}\cdot\frac{V_p}{V_T} - 1. \qquad (2)$$

Assuming that the protein is a sphere with a radius of gyration of ~3 nm (45,46), we deduce corrected α_{relative} values for each protein concentration using Eq. 2. Assuming a transparent nonabsorbing protein ($\alpha_p \approx 0$ cm^{-1}), we predict a linear decrease of α_{relative} with increasing protein concentration, as is plotted in Fig. 2 (*dotted line*). In a more realistic case, where the protein has an absorption coefficient $0 < \alpha_p < \alpha_b$, we still expect a linear concentration dependence with a slope which is increased compared to the dotted line in Fig. 2. The experimentally determined THz absorption relative to buffer of the solvated protein clearly deviates from this predicted α_{relative}. Such deviations from a linear two-component model have also been found for other proteins such as λ-repressor (17), ubiquitin (19), and anti-freeze (47). We attribute this observed nonlinear behavior to the contribution of a third component, i.e., the water in the dynamical hydration shell around the protein. Water within the dynamical hydration shell is assumed to have an increased THz absorption coefficient compared to bulk water.

In Fig. 2, we compare the results of the concentration-dependent THz absorption measurements for different temperatures. For a comparison, we have to keep in mind that a change in temperature goes along with structural changes of the protein itself. As a general trend, we find a decrease of the THz absorption relative to buffer with increasing temperature. It is to be noted here that CD measurements show a considerable rupture of both secondary and tertiary structure of the protein during E→U transition as the temperature is raised to 70°C (Fig. 1), coupled with a twofold increase in the size of the hydrated protein as observed from dynamic light scattering (DLS) measurements (36,48). At the thermal unfolded state at 70°C, an increase in the protein volume leads to a decrease in THz absorption (by an increased THz defect).

Fig. 3 summarizes the observed change in the THz absorption relative to buffer of 1 mM HSA solution in the two unfolding-refolding pathways (Process 1 and 2). For a comparison, we also plot the absorption coefficient of the buffer in the inset of Fig. 3 *A*. In this THz frequency range, the absorption of buffer (water) is high and increases linearly with temperature. As shown in Fig. 3 *A*, we find a reversible change of absorption for the N→E unfolding pathway, e.g., the refolded protein shows almost the same THz absorption as the native one. However, the scenario is quite different for the N→U transition (Fig. 3 *B*). Here, the absorption relative to buffer of the refolded protein is distinct from that of the native protein, which clearly points to a substantial irreversible modification of hydration dynamics.

THz spectroscopy can probe the long-range collective water network motions extending over several hydration shells (23), which are inaccessible by other techniques. It can thus report on subtle changes in the collective hydrogen-bond network dynamics of the hydration layer. CD experiments (Fig. 1) clearly suggest moderate and considerable modification of the protein secondary and tertiary structure for the N→E and N→U transitions, respectively. DLS probes hydration on the microsecond-to-millisecond timescale. There we find for the first process, a negligible, and for the second process, a twofold change in the hydrodynamic diameter (d_h) of HSA (36). The increase in d_h is attributed to the equilibrium volume expansion of the protein upon thermal denaturation. The THz absorption measurements, on the other hand, probe changes in the coupled protein-solvent dynamics on a picosecond timescale. Earlier studies have concluded that during the N→E transition, buried residues of HSA get exposed without significantly damaging the protein structure (35,36), which can perturb the long-range solute-solvent interaction.

With a combination of molecular-dynamics simulation studies and experimental results, we could show that the vibrational density of states of water molecules in the hydration shell of a protein is blue-shifted compared to bulk water (27). This is attributed to a significant retardation of hydrogen-bond dynamics on a picosecond timescale. This retardation also goes along with a retardation of the rotational motions of water molecules and diffusion times. Although this retardation effect is less surprising for water molecules at hydrophilic residues (which can form hydrogen bonds to the nearby water molecules), the effect is also present for water molecules in the vicinity of hydrophobic residues. A closer look revealed that the observed effect for hydrophobic residues is mostly caused by sterical hindrance effects, because hydrophobic residues are buried in pockets, grooves, and clefts. Any retardation of water network dynamics is found to cause a blue shift of the vibrational density of states. The blue shift is connected with an increase in THz absorption for frequency above 1.7 THz (e.g., between 2.1 and 2.8 THz) and a decrease in THz absorption for frequency below 1.7 THz compared to the bulk value.

If the sterical constraints posed on water molecules are relieved due to an N→E or even due to an N→U transition, we expect a smaller blue shift. The observed change in THz absorption is therefore directly related to the fraction of solvation water molecules in grooves or in other sterically demanding environments. Following our theoretical prediction, we propose that the water molecules within the dynamical hydration shell of folded protein will show a significant retardation of hydrogen-bond dynamics, whereas the E and U states impose less effect on the surrounding water network.

The refolding results of the protein (Fig. 3) can be explained in the light of these predictions. As observed from Fig. 3 *A*, the E state refolds almost perfectly to the native state as the absorption relative to buffer suffers minimal deviation upon unfolding. This transition thus proves to be efficient (kinetically) as well as inexpensive (thermodynamically). For the N→U transition, we find an increased absorption for the final state compared to the initial native state. Both CD and DLS experiments provide evidence of a structurally disordered U state in which some of the HSA subdomains melt to expose their hydrophobic core to the solvent. Such hydrophobic hydration produces a blue shift in the vibrational density of states of oxygen, thus increasing the density in the 2.4 THz frequency region (27). The associated change in conformational entropy during structural perturbation, which favors the unfolding process, is supported by an energy cost from S-S bond cleavage in the U state as evidenced from the near-UV CD spectra (49,50). This entropic change is perhaps not recovered upon the depletion of water during the refolding process and results in an improperly folded state exposing the hydrophobic solute residues, which causes an increased absorption for the refolded state.

In addition, we measured the THz-TDS for 1 mM HSA aqueous solution in a frequency range of 0.1–1.2 THz at different temperatures. For each measurement, we recorded the time-dependent electric field of the transmitted THz pulses for empty cell (reference) and filled cell (sample). A fast Fourier transform was applied to the time-domain data to obtain the frequency-dependent power $I(\nu)$ and phase $\phi(\nu)$ of the transmitted THz pulses (51). From these data, we deduced the frequency-dependent absorption coefficient $\alpha(\nu)$ (power attenuation) according to Eq. 3, and the frequency-dependent index of refraction $n(\nu)$ (delay of the THz pulses) according to Eq. 4,

$$\alpha(\nu) = \frac{\ln I_o(\nu) - \ln I_s(\nu)}{d}, \tag{3}$$

$$n(\nu) = \frac{\phi_s(\nu) - \phi_o(\nu)}{2\pi\nu d}\cdot c + 1, \tag{4}$$

where d is the thickness of the liquid cell, c is the light velocity, and the indices *0* and *s* represent the measured data of the reference cell and sample cell, respectively. Fig. 4, *A* and *B*, shows $\alpha(\nu)$ and $n(\nu)$ for buffer and aqueous HSA solution at 20°C and 70°C. The curves for the buffer solution at room temperature resemble the previously

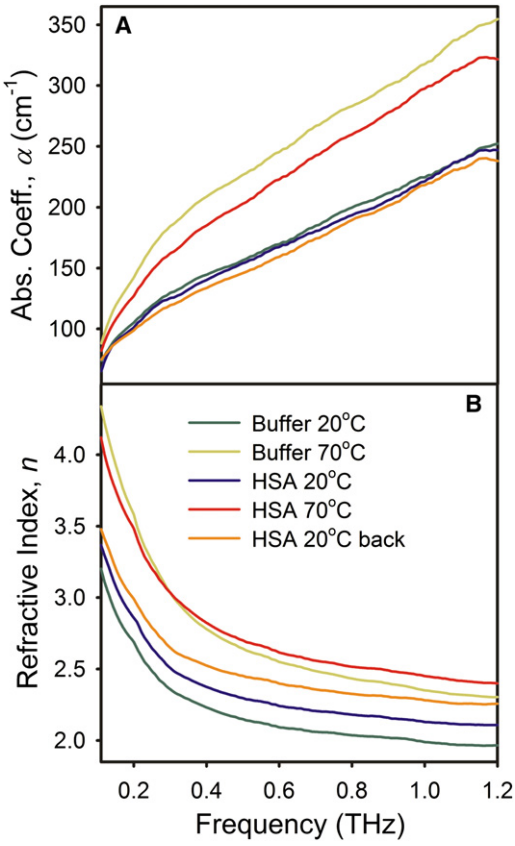

FIGURE 4 THz-TDS spectra of PBS buffer (pH 7.4) and 1 mM HSA in PBS buffer at 20°C and 70°C in the range from 0.1 to 1.2 THz: displayed is the absorption coefficient (*A*), and refractive index (*B*).

reported results (52). The absorption coefficient changes from 80 cm^{-1} to 240 cm^{-1} in the investigated frequency window, which is in excellent agreement with that reported by Thrane et al. (53) for water at 292 K. As the temperature is increased to 70°C, both $\alpha(\nu)$ and $n(\nu)$ of the buffer increase and absorption changes from 90 to 350 cm^{-1} in the frequency window, which is in good agreement with the results of Zelsmann (54), who reported temperature-dependent absorption of water.

In accordance with our general predictions (27) we find an increased THz absorption with increasing frequency between 0.1 and 1.2 THz, and a decreased THz absorption for the protein solution compared to that of buffer. Similar to the measurement at 2.1–2.8 THz, for the N→E transition, $n(\nu)$ and $\alpha(\nu)$ resemble the values for the native state when the system is allowed to refold (data not shown). For refolding from the U state, we observe an irreversible transition. Whereas for the p-Ge measurements, the absorption of the refolded protein in Process 2 at 20°C is found to be increased compared to the native protein at 20°C, for the THz-TD measurements we find a decreased THz absorption coefficient.

For fluorescence spectroscopy, HSA has a single Trp moiety in the 214 position which produces an absorption peak at ~280 nm. When we excite the protein at 300 nm to avoid fluorescence from other emitting amino acids, we obtain the emission spectrum as shown in Fig. 5 *A*. The protein shows a single emission peak at 335 nm at room temperature. For Process 1, with increasing temperature the emission peak intensity decreases; however, the emission maximum position (λ_{max}) remains almost unchanged when heated up to 55°C (Fig. 5 *A*, *lower inset*). The observed quenching of emission intensity is attributed to a decreased quantum yield of Trp in its immediate environment. Upon cooling, the fluorescence intensity is increasing and at room temperature the emission spectrum (*dashed line*) reproduces almost exactly that of the native state spectrum (Fig. 5 *A*, *lower inset*). A small reversible change in the position of the maximum absorption (λ_{max}) is in agreement with near-UV CD spectra.

A markedly different observation is found for Process 2. When the temperature is increased to 70°C, a distinct 4–5 nm blue shift of the emission peak position (λ_{max}) is found coupled with a decrease in the emission intensity. Previously, Shaw and Pal (48) also reported such blue shift of HSA emission at elevated temperatures. In the U state transition domain II of the protein unfolds in such a way that Trp^{214} residue of HSA located at the bottom of a 12 Å deep crevice (55,56) finds itself in a more hydrophobic environment. This blue shift indicates an increased exposure of hydrophobic moiety to the protein surface as has also been found in the THz absorption studies. Fig. 5 *A* (*higher inset*, *dashed line*) shows the change upon subsequent cooling. The blue-shifted emission spectrum of the refolded state of the protein marks an irreversible rupture of the secondary

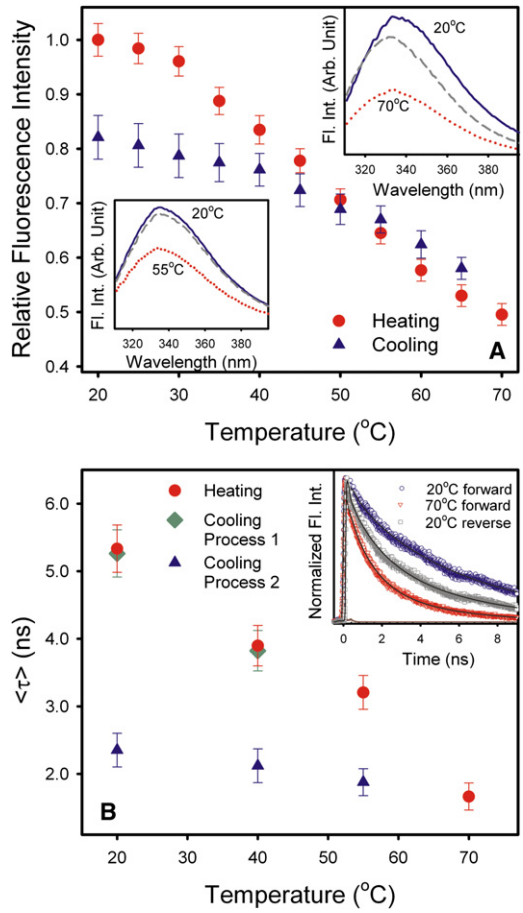

FIGURE 5 (*A*) Change in the relative intensity of the Trp emission maximum of HSA during thermal unfolding and refolding processes. (*Insets*) Total spectra at different temperatures. (*Dashed lines* at 20°C) Spectrum of the refolded species. (*B*) Average lifetime of ($\langle\tau\rangle$) of Trp in HSA at different temperatures during thermal unfolding and refolding for Processes 1 and 2. Inset shows spectra of the native state (20°C forward), unfolded state (70°C forward), and refolded state of process 2 (20°C reverse), respectively.

and tertiary structure of the protein upon refolding which is not recovered upon cooling. This trend is also observed when we plot the relative emission peak intensity for both the heating and cooling processes for Process 2 (Fig. 5 *A*).

Furthermore, we have measured the lifetime of Trp emission of HSA at different temperatures. The fluorescence transients are fitted to a triexponential curve (Fig. 5 *B*) and the fitting parameters are given in Table 1. As observed from the table, at room temperature the fitted lifetimes are 0.5, 3.3, and 7 ns. The most dominant contribution of the longer component corresponds to an average lifetime ($\langle\tau\rangle$) of 5.2 ns. The obtained results are in good agreement with previous reports (57,58). It is to be noted here that the observed decay dynamics of Trp in HSA is significantly slower than that of aqueous Trp which can be fitted to a biexponential curve with fitted lifetimes of 0.5 and 2.8 ns, of which the latter component dominates (59). It is interesting

TABLE 1 Fitting parameters of the decay transients of Trp emission in HSA with temperatures

T (°C)	a_1	τ_1 (ns)	a_2	τ_2 (ns)	a_3	τ_3 (ns)	$\langle\tau\rangle$ (ns)
Heating up to 70°C followed by cooling							
Unfolding							
20	0.15	0.50	0.21	3.31	0.64	7.00	5.23
40	0.22	0.34	0.26	2.34	0.52	5.85	3.76
55	0.21	0.25	0.44	2.30	0.35	5.50	2.99
70	0.24	0.15	0.48	1.18	0.28	3.76	1.66
Refolding							
55	0.35	0.14	0.38	1.57	0.27	4.52	1.88
40	0.37	0.14	0.31	1.59	0.32	4.90	2.12
20	0.38	0.12	0.26	1.58	0.36	5.30	2.35
Refolding from 55°C							
40	0.19	0.30	0.30	2.40	0.51	5.99	3.82
20	0.12	0.45	0.28	3.21	0.60	7.22	5.26

to note that these two components are found in most of the Trp-containing proteins (60).

In this study, we find an additional component with a lifetime of 7 ns, which is characteristic of the hydrophobic environment experienced by buried Trp, as has also been previously observed in water-alcohol mixture (59). At normal physiological condition, the heart-shaped N-form of the protein adopts a globular structure (55,56). This quenching in lifetime is a consequence of the release of core water upon unfolding which has already been manifested in the change of hydration dynamics as observed by THz measurements. Trp^{214} sits in a 12 Å deep water-filled crevice in domain IIA of HSA. The trapped water molecules in these binding pockets are in dynamic equilibrium with bulk water (61) and this additional constraint on the Trp moiety might give rise to the additional 7 ns component. With increasing temperature, as the secondary and tertiary structure of the protein unfolds, the contribution of the long component decreases continuously for the N→E transition and significantly for the E→U transition, resulting in an approximately threefold decrease in $\langle\tau\rangle$ (Table 1, Fig. 5 *B*). When the system is allowed to cool from 55°C, the $\langle\tau\rangle$ value is recovered completely, whereas when cooled from the U state at 70°C, only a fraction of the native value is recovered (Table 1, Fig. 5 *B*).

CONCLUSIONS

We present here a combined fluorescence/THz study of the solvated HSA protein. Far- and near-UV CD spectroscopy indicates a marginal change in the secondary and tertiary structure of the protein during N→E transition for heating up to 55°C and a dramatic change during E→U transitions for heating beyond 70°C. The associated change in the solvation is studied using THz and fluorescence spectroscopy. Precise measurements of the THz absorption of solvated HSA proteins show significant deviation from a two-component model. This can be explained by an increased THz absorption for water in the dynamical hydration shell of the protein. The measurements indicate a blue shift of the THz absorption spectrum of the solvated HSA protein compared to bulk water, which can be correlated on the molecular scale with a change in the fast collective solvation dynamics in the vicinity of the protein.

Upon unfolding of the protein, we find an increased exposure of hydrophobic side chains to the solvent. However, the sterical constraints posed on water molecules are expected to be significantly relieved upon a destabilization and increase of flexibility compared to the native protein structure. Because any retardation due to sterical constraints (such as apply for water in hydrophobic pockets and grooves) causes a blue shift in the vibrational density of states, any relief of sterical constraints is expected to shift the vibrational density of states to a more bulklike spectrum. This explains the fact that in Fig. 2 the unfolded state (U at °C) approaches more a linear, two-component model, as well as the fact that the refolded protein has a smaller deviation from the bulk THz absorption than the folded protein (Fig. 3).

How do we explain the change of the THz absorption as observed by THz time domain spectroscopy? Here we expect a decrease in the THz absorption for a folded, more structured protein compared to an unfolded protein. This prediction is confirmed when we take the difference between the THz absorption for an unfolded protein (HSA unfolded) compared to a folded solvated protein at 20°C (see Fig. 4 *A*). Fig. 4 *A* shows that whereas the native and the refolded protein agree within experimental accuracy, for the unfolded protein at 70°C we find a significantly increased THz absorption coefficient compared to the THz absorption coefficient at 20°C. However, if we compare this value to the bulk spectrum of water at 70°C (and not at 20°C), we see that the THz absorption is still decreased. Therefore, we find here three different processes which contribute to the observed changes in the coupled protein-water network dynamics as probed by THz absorption spectroscopy:

Process 1. The increase in temperature results in a general change of the bulk water network dynamics which is known to yield an overall increased THz absorption coefficient over the entire frequency range (0–3 THz).

Process 2. The change of the exposure of protein side chains to the solvent causes a change in the THz absorption coefficient of the water in the dynamical hydration shell of the protein.

Process 3. Due to exclusion of water molecules by the less absorbing protein, we expect a "THz defect", i.e., a decrease of THz absorption with increasing protein concentration.

Whereas Process 1 is expected to lead to an increase in THz absorption of bulk water, or buffer solution, the water in the dynamical hydration shell is expected to show a decreased THz absorption coefficient compared to bulk

water. An increased protein volume as expected for the unfolded state would also cause a decrease in THz absorption. So, some of the changes will cancel and an overall subtle balance between different contributions will be found, which makes a direct comparison difficult.

When heating to 70°C, the protein is found to be in the U state. This process is irreversible, i.e., remaining structural changes are found when the protein is cooled down to 20°C. These structural changes are accompanied by irreversible changes in the hydration dynamics as observed by THz absorption spectroscopy in the entire frequency range. Our conclusions are supported by additional CD and fluorescence measurements. The reported measurements show a clear correlation between structural changes and changes in the hydration dynamics for the HSA protein.

REFERENCES

1. Ball, P. 2008. Water as an active constituent in cell biology. *Chem. Rev.* 108:74–108.
2. Pal, S. K., and A. H. Zewail. 2004. Dynamics of water in biological recognition. *Chem. Rev.* 104:2099–2123.
3. Pal, S. K., J. Peon, …, A. H. Zewail. 2002. Biological water: femtosecond dynamics of macromolecular hydration. *J. Phys. Chem. B.* 106:12376–12395.
4. Chaplin, M. 2006. Do we underestimate the importance of water in cell biology? *Nat. Rev. Mol. Cell Biol.* 7:861–866.
5. Halle, B. 2004. Protein hydration dynamics in solution: a critical survey. *Philos. Trans. R. Soc. Lond. B Biol. Sci.* 359:1207–1223, discussion 1223–1224, 1323–1328.
6. Frauenfelder, H., P. W. Fenimore, …, B. H. McMahon. 2006. Protein folding is slaved to solvent motions. *Proc. Natl. Acad. Sci. USA.* 103:15469–15472.
7. Fenimore, P. W., H. Frauenfelder, …, F. G. Parak. 2002. Slaving: solvent fluctuations dominate protein dynamics and functions. *Proc. Natl. Acad. Sci. USA.* 99:16047–16051.
8. Tanford, C. 1980. The Hydrophobic Effect: Formation of Micellar and Biological Membranes. Wiley Interscience, New York.
9. Bakk, A., J. S. Høye, and A. Hansen. 2002. Apolar and polar solvation thermodynamics related to the protein unfolding process. *Biophys. J.* 82:713–719.
10. Robinson, G. W., and C. H. Cho. 1999. Role of hydration water in protein unfolding. *Biophys. J.* 77:3311–3318.
11. Makhatadze, G. I., and P. L. Privalov. 1994. Hydration effects in protein unfolding. *Biophys. Chem.* 51:291—309..
12. Oobatake, M., and T. Ooi. 1993. Hydration and heat stability effects on protein unfolding. *Prog. Biophys. Mol. Biol.* 59:237–284.
13. Levy, Y., and J. N. Onuchic. 2006. Water mediation in protein folding and molecular recognition. *Annu. Rev. Biophys. Biomol. Struct.* 35:389–415.
14. Sorenson, J. M., G. Hura, …, T. Head-Gordon. 1999. Determining the role of hydration forces in protein folding. *J. Phys. Chem. B.* 103:5413–5426.
15. Ebbinghaus, S., K. Schröck, …, M. Havenith. 2006. Terahertz time-domain spectroscopy as a new tool for the characterization of dusty plasmas. *Plasma Sources Sci. Technol.* 15:72–77.
16. Ebbinghaus, S., S. J. Kim, …, M. Havenith. 2007. An extended dynamical hydration shell around proteins. *Proc. Natl. Acad. Sci. USA.* 104:20749–20752.
17. Ebbinghaus, S., S. J. Kim, …, M. Havenith. 2008. Protein sequence- and pH-dependent hydration probed by terahertz spectroscopy. *J. Am. Chem. Soc.* 130:2374–2375.
18. Heyden, M., E. Bründermann, …, M. Havenith. 2008. Long-range influence of carbohydrates on the solvation dynamics of water—answers from terahertz absorption measurements and molecular modeling simulations. *J. Am. Chem. Soc.* 130:5773–5779.
19. Born, B., S. J. Kim, …, M. Havenith. 2009. The terahertz dance of water with the proteins: the effect of protein flexibility on the dynamical hydration shell of ubiquitin. *Faraday Discuss.* 141:161–173, discussion 175–207.
20. Born, B., H. Weingärtner, …, M. Havenith. 2009. Solvation dynamics of model peptides probed by terahertz spectroscopy. Observation of the onset of collective network motions. *J. Am. Chem. Soc.* 131: 3752–3755.
21. Walrafen, G. E. 1990. Raman spectrum of water: transverse and longitudinal acoustic modes below $\approx$300 cm^{-1} and optic modes above $\approx$300 cm^{-1}. *J. Phys. Chem.* 94:2237–2239.
22. Hasted, J. B., S. K. Husain, …, J. R. Birch. 1985. Far-infrared absorption in liquid water. *Chem. Phys. Lett.* 118:622–625.
23. Heyden, M., J. Sun, …, D. Marx. 2010. Dissecting the THz spectrum of liquid water from first principles via correlations in time and space. *Proc. Natl. Acad. Sci. USA.* 107:12068–12073.
24. Markelz, A. G., A. Roitberg, and E. J. Heilweil. 2000. Pulsed terahertz spectroscopy of DNA, bovine serum albumin and collagen between 0.1 and 2.0 THz. *Chem. Phys. Lett.* 320:42–48.
25. Png, G. M., R. J. Falconer, …, D. Abbott. 2009. Terahertz spectroscopic differentiation of microstructures in protein gels. *Opt. Express.* 17:13102–13115.
26. Heugen, U., G. Schwaab, …, M. Havenith. 2006. Solute-induced retardation of water dynamics probed directly by terahertz spectroscopy. *Proc. Natl. Acad. Sci. USA.* 103:12301–12306.
27. Heyden, M., and M. Havenith. 2010. Combining THz spectroscopy and MD simulations to study protein-hydration coupling. *Methods.* 52:74–83.
28. Kragh-Hansen, U., V. T. G. Chuang, and M. Otagiri. 2002. Practical aspects of the ligand-binding and enzymatic properties of human serum albumin. *Biol. Pharm. Bull.* 25:695–704.
29. He, X. M., and D. C. Carter. 1992. Atomic structure and chemistry of human serum albumin. *Nature.* 358:209–215.
30. Sugio, S., A. Kashima, …, K. Kobayashi. 1999. Crystal structure of human serum albumin at 2.5 Å resolution. *Protein Eng.* 12:439–446.
31. Michnik, A., K. Michalik, …, Z. Drzazga. 2006. Comparative DSC study of human and bovine serum albumin. *J. Therm. Anal. Calorim.* 84:113–117.
32. Baranov, A. N., I. M. Vlasova, …, A. M. Saletskii. 2004. Laser correlation spectroscopy of the processes of serum albumin denaturation. *J. Appl. Spectrosc.* 71:911–915.
33. Picó, G. A. 1997. Thermodynamic features of the thermal unfolding of human serum albumin. *Int. J. Biol. Macromol.* 20:63–73.
34. Sinha, S. S., R. K. Mitra, and S. K. Pal. 2008. Temperature-dependent simultaneous ligand binding in human serum albumin. *J. Phys. Chem. B.* 112:4884–4891.

35. Flora, K., J. D. Brennan, …, F. V. Bright. 1998. Unfolding of acrylodan-labeled human serum albumin probed by steady-state and time-resolved fluorescence methods. *Biophys. J.* 75:1084–1096.

36. Mitra, R. K., S. S. Sinha, and S. K. Pal. 2007. Hydration in protein folding: thermal unfolding/refolding of human serum albumin. *Langmuir.* 23:10224–10229.

37. Wu, Y., B. Czarnik-Matusewicz, …, Y. Ozaki. 2000. Two-dimensional near-infrared spectroscopy study of human serum albumin in aqueous solutions. *J. Phys. Chem. B.* 104:5840–5847.

38. Wetzel, R., M. Becker, …, G. Lassmann. 1980. Temperature behavior of human serum albumin. *Eur. J. Biochem.* 104:469–478.

39. Dockal, M., D. C. Carter, and F. Rüker. 1999. The three recombinant domains of human serum albumin. Structural characterization and ligand binding properties. *J. Biol. Chem.* 274:29303–29310.

40. Dockal, M., D. C. Carter, and F. Rüker. 2000. Conformational transitions of the three recombinant domains of human serum albumin depending on pH. *J. Biol. Chem.* 275:3042–3050.

41. Moriyama, Y., and K. Takeda. 2005. Protective effects of small amounts of bis(2-ethylhexyl)sulfosuccinate on the helical structures of human and bovine serum albumins in their thermal denaturations. *Langmuir.* 21:5524–5528.

42. Uversky, V. N., N. V. Narizhneva, …, A. Y. Tomashevski. 1997. Rigidity of human α-fetoprotein tertiary structure is under ligand control. *Biochemistry.* 36:13638–13645.

43. Era, S., K. B. Itoh, …, H. Watari. 1990. Structural transition of bovine plasma albumin in the alkaline region—the N-B transition. *Int. J. Pept. Protein Res.* 35:1–11.

44. Sogami, M., S. Era, …, H. Inouye. 1982. Circular dichroic and fluoropolarimetric studies on tryptophyl residues in acid-induced isomerization of bovine plasma albumin. *Int. J. Pept. Protein Res.* 19:263–269.

45. Galantini, L., C. Leggio, and N. V. Pavel. 2008. Human serum albumin unfolding: a small-angle x-ray scattering and light scattering study. *J. Phys. Chem. B.* 112:15460–15469.

46. Olivieri, J. R., and A. F. Craievich. 1995. The subdomain structure of human serum albumin in solution under different pH conditions studied by small angle x-ray scattering. *Eur. Biophys. J.* 24:77–84.

47. Ebbinghaus, S., K. Meister, …, M. Havenith. 2010. Antifreeze glycoprotein activity correlates with long-range protein-water dynamics. *J. Am. Chem. Soc.* 132:12210–12211.

48. Shaw, A. K., and S. K. Pal. 2008. Spectroscopic studies on the effect of temperature on pH-induced folded states of human serum albumin. *J. Photochem. Photobiol. B.* 90:69–77.

49. Cheung, M. S., A. E. García, and J. N. Onuchic. 2002. Protein folding mediated by solvation: water expulsion and formation of the hydrophobic core occur after the structural collapse. *Proc. Natl. Acad. Sci. USA.* 99:685–690.

50. Baldwin, R. L. 1986. Temperature dependence of the hydrophobic interaction in protein folding. *Proc. Natl. Acad. Sci. USA.* 83:8069–8072.

51. Kindt, J. T., and C. A. Schmuttenmaer. 1996. Far-infrared dielectric properties of polar liquids probed by femtosecond terahertz pulse spectroscopy. *J. Phys. Chem.* 100:10373–10379.

52. Zhang, C., and S. M. Durbin. 2006. Hydration-induced far-infrared absorption increase in myoglobin. *J. Phys. Chem. B.* 110:23607–23613.

53. Thrane, L., R. H. Jacobsen, …, S. R. Keiding. 1995. THz reflection spectroscopy of liquid water. *Chem. Phys. Lett.* 240:330–333.

54. Zelsmann, H. R. 1995. Temperature dependence of the optical constants for liquid H_2O and D_2O in the far IR region. *J. Mol. Struct.* 350:95–114.

55. Curry, S., H. Mandelkow, …, N. Franks. 1998. Crystal structure of human serum albumin complexed with fatty acid reveals an asymmetric distribution of binding sites. *Nat. Struct. Biol.* 5:827–835.

56. Zunszain, P. A., J. Ghuman, …, S. Curry. 2003. Crystal structural analysis of human serum albumin complexed with hemin and fatty acid. *BMC Struct. Biol.* 3:6.

57. Vos, K., A. van Hoek, and A. J. W. G. Visser. 1987. Application of a reference convolution method to tryptophan fluorescence in proteins. A refined description of rotational dynamics. *Eur. J. Biochem.* 165: 55–63.

58. Siemiarczuk, A., C. E. Petersen, …, N. V. Bhagavan. 2004. Analysis of tryptophan fluorescence lifetimes in a series of human serum albumin mutants with substitutions in subdomain 2A. *Cell Biochem. Biophys.* 40:115–122.

59. Albani, J. R. 2009. Fluorescence lifetimes of tryptophan: structural origin and relation with So $\rightarrow$ 1Lb and So $\rightarrow$ 1La transitions. *J. Fluoresc.* 19:1061–1071.

60. Albani, J. R. 2007. New insights in the interpretation of tryptophan fluorescence. Origin of the fluorescence lifetime and characterization of a new fluorescence parameter in proteins: the emission to excitation ratio. *J. Fluoresc.* 17:406–417.

61. Qiu, W., L. Zhang, …, A. H. Zewail. 2006. Ultrafast solvation dynamics of human serum albumin: correlations with conformational transitions and site-selected recognition. *J. Phys. Chem. B.* 110: 10540–10549.